A New Magnetic Lattice in the "Cdta Family". Structure and Magnetic Properties of the Novel Homo- and Heterometallic Chains $Cu_3[M(cdta)]_2(NO_3)_2 \cdot 15H_2O$ (M = Cu, Ni)

F. Sapiña,[1a] E. Escrivá,[1a] J. V. Folgado,[1a] A. Beltrán,[1a] D. Beltrán,*[1a] A. Fuertes,[1b] and M. Drillon[1c]

Departament de Química Inorgànica (UIBCM), Facultat de Ciències Químiques, Universitat de València, c/Dr. Moliner 50, 46100 Burjassot, València, Spain, Institut de Ciencia de Materials (CSIC), 08193 Bellaterra, Barcelona, Spain, and Group de Chimie des Matériaux Inorganiques, EHICS, 1 rue Blaise Pascal, 67008 Strasbourg, France

Received August 6, 1991

The structure of $Cu_3[Ni(cdta)]_2(NO_3)_2 \cdot 15H_2O$ (**1**) and $Cu_3[Cu(cdta)]_2(NO_3)_2 \cdot 15H_2O$ (**2**) (cdta = *trans*-cyclohexane-1,2-diamine-*N*,*N*,*N*′,*N*′-tetraacetate) has been determined by X-ray methods. Both isostructural compounds crystallize in the monoclinic space group $I2/a$ with $Z = 4$ in cells of dimensions $a = 21.419$ (4) Å, $b = 7.806$ (3) Å, $c = 30.156$ (6) Å, and $\beta = 90.36$ (2)° for **1** and $a = 21.404$ (6) Å, $b = 7.742$ (2) Å, $c = 30.712$ (5) Å, and $\beta = 90.99$ (2)° for **2**. Least-squares refinement of 3390 (**1**) and 2930 (**2**) reflections [$I > 2.5\sigma(I)$] and 346 parameters (in both cases) gave a final R of 0.037 for **1** and 0.046 for **2**. The complexes are built up of two different "hydrated" (square-planar and square-pyramidal) and one "chelated" (octahedral) coordination entities, which are bridged through carboxylate groups. Whereas the chelated position may indistinctly be occupied by nickel(II) or copper(II) ions, both hydrated sites are exclusively occupied by copper(II) ions. The connectivity among the coordination polyhedra leads to infinite chains ...$[M(cdta)]$...$[O_{III}Cu(OH_2)_2O_{III}]$...$[M(cdta)]$...$[O_ICu(OH_2)_3O_{II}]_2$...$[M(cdta)]$... parallel to [001], where the [M(cdta)] units share three carboxylate groups with the cationic entities. Magnetic susceptibility measurements in the range 1.8–250 K are discussed in terms of an Ising model. These novel systems give rise to a new kind of one-dimensional magnetic network built up from three magnetic sublattices connected through three different interactions. In compound **2** the magnetic behavior is satisfactorily interpreted on the basis of the structural features of the bridging network and coordination sites. On the contrary, the observed behavior for compound **1** (which is strongly influenced by the local anisotropy of Ni(II) ions) cannot be easily correlated with the crystal structure.

Introduction

The characterization of a wide set of families of structurally ordered bimetallic derivatives has been one of the main factors contributing to the recent progress in magnetochemistry.[2] These systems contain two or more different coordination sites that may selectively be occupied on the basis of their chemical and structural features. This implies the possibility of built up chemically controlled ordered arrays of metallic atoms in a lattice.[3]

Indeed, we have previously benefited from the chelating ability of ligands such as edta (ethylenediamine-*N*,*N*,*N*′,*N*′-tetraacetate) and cdta (*trans*-cyclohexane-1,2-diamine-*N*,*N*,*N*′,*N*′-tetraacetate) to obtain a versatile series of bimetallic materials (i.e., the so-called edta and cdta families) in which the ordered disposition of the cations results in a very rich magnetochemistry.[4-7] Both the order and its diversity arise as a consequence of the availability—after the formation of a stable anionic $[ML]^{2-}$ species in solution—of one or more carboxylate groups that may act as bridging entities toward another $M^{2+}(aq)$ cation. Thus, dimers are obtained when only one carboxylate group per ligand acts as a bridge.[4] The presence of two carboxylate bridges may yield both tetramers[5] and linear chains.[6] This last series constitutes one of the more versatile families of ferrimagnetic systems known up to now.[3] In the case of edta, the synthesis conditions under relatively high temperature, pressure and concentration favored a higher connectivity between the metallic cations (i.e., there were four carboxylate bridging groups) in such a way that polymeric 3-D ferrimagnetic materials resulted.[7]

In the present work we report the serendipitous results obtained when conditions of relatively high concentration and smooth temperature were applied to the synthesis of bimetallic (Cu, Ni) derivatives of cdta. We describe the synthesis, structure, and magnetic properties of a new series of compounds of formula $Cu_3[Cu_{1-x}Ni_x(cdta)]_2(NO_3)_2 \cdot 15H_2O$ ($0 \le x \le 1$) in which the connectivity between the metallic atoms is established through three carboxylate groups.

Experimental Section

Preparation of the $Cu_3[Cu_{1-x}Ni_x(cdta)]_2(NO_3)_2 \cdot 15H_2O$ Compounds. $Cdta^{4-}$ aqueous solutions (0.220 mol·L^{-1}) were prepared as described in ref 8. Nickel-containing compounds (**1**, $x = 1$; **3**, $x = 0.5$) were prepared by adding solid $Ni(NO_3)_2 \cdot 6H_2O$ (**1**, 2.75 mmol; **3**, 5.50 mmol) to a portion of 25 mL of the $cdta^{4-}$ solution while the mixture was stirred. After a period of time (during which the stirring was maintained) to ensure $[Ni(cdta)]^{2-}$ formation, solid $Cu(NO_3)_2 \cdot 3H_2O$ (**1**, 8.25 mmol; **3**, 11.00 mmol) was added while the mixture was stirred. The copper compound (**2**, $x = 0$) was prepared by adding solid $Cu(NO_3)_2 \cdot 3H_2O$ (13.75 mmol) to another 25-mL portion of the $cdta^{4-}$ solution while the mixture was stirred. In all three cases, the molar ratio of metal (Cu + Ni) to cdta was maintained constant and equal to 2.50. The pH values of the resulting

(1) (a) Universitat de València. (b) Institut de Materials. (c) EHICS.
(2) Kahn, O. *Struct. Bonding (Berlin)* **1987**, *68*, 89.
(3) Landee, C. P. In *Organic and Inorganic Low Dimensional Crystalline Materials*; Delhaes, P., Drillon, M., Eds.; NATO ASI Series 168; Plenum Press: New York, 1987; p 75.
(4) (a) Fuertes, A.; Miravitlles, C.; Escrivá, E.; Coronado, E.; Beltrán, D. *J. Chem. Soc., Dalton Trans.* **1987**, 1847. (b) Fuertes, A.; Miravitlles, C.; Molins, E.; Escrivá, E.; Beltrán, D. *Acta Crystallogr.* **1986**, *C42*, 421.
(5) Fuertes, A.; Miravitlles, C.; Escrivá, E.; Coronado, E.; Beltrán, D.; Padel, L. *J. Chem. Soc., Dalton Trans.* **1989**, 863.
(6) (a) Coronado, E.; Drillon, M.; Fuertes, A.; Beltrán, D.; Mosset, A.; Galy, J. L. *J. Am. Chem. Soc.* **1986**, *108*, 900. (b) Fuertes, A.; Miravitlles, C.; Escrivá, E.; Coronado, E.; Beltrán, D. *J. Chem. Soc., Dalton Trans.* **1986**, 1795. (c) Solans, X.; Font Altaba, M. *Eur. Cryst. Meeting* **1982**, *7*, 201. (d) Mosset, A.; Galy, J.; Muñoz-Roca, C.; Beltrán-Porter, D. *Z. Kristall.* **1987**, *181*, 83.
(7) (a) Gomez-Romero, P.; Jameson, G. B.; Casañ-Pastor, N.; Coronado, E.; Beltrán, D. *Inorg. Chem.* **1986**, *25*, 3171. (b) Sapiña, F.; Coronado, E.; Beltrán, D.; Burriel, R. *J. Am. Chem. Soc.* **1991**, *113*, 7940.
(8) Fuertes, A.; Escrivá, E.; Muñoz, M. C.; Alamo, J.; Beltrán, A.; Beltrán, D. *Transition Met. Chem.* **1987**, *12*, 62.

0020-1669/92/1331-3851$03.00/0

Table I. Analytical Data for the Complexes $Cu_3[Cu_{1-x}Ni_x(cdta)]_2(NO_3)_2 \cdot 15H_2O$

compd	% found (% calcd)				
	Cu	Ni	C	H	N
1	13.8 (13.7)	8.3 (8.5)	24.6 (24.3)	4.0 (4.8)	6.2 (6.1)
2	18.3 (18.3)	4.0 (4.2)	24.3 (24.2)	4.3 (4.8)	5.9 (6.0)
3	22.4 (22.8)		23.3 (24.1)	4.3 (4.7)	6.0 (6.0)

Table II. Crystallographic Data for Compounds **1** and **2**

	1	**2**
chem formula	$C_{28}H_{66}Cu_3Ni_2N_6O_{37}$	$C_{28}H_{66}Cu_5N_6O_{37}$
fw	1386.88	1396.53
space group	*I*2/*a*	*I*2/*a*
Z	4	4
a, Å	21.419 (4)	21.404 (6)
b, Å	7.806 (3)	7.742 (2)
c, Å	30.156 (6)	30.712 (5)
β, deg	90.36 (2)	90.99 (2)
V, Å^3	5042 (1)	5089 (1)
ρ_{obs} (ρ_{calc}), g cm^{-3}	1.81 (1.83)	1.82 (1.83)
μ(Mo Kα), cm^{-1}	20.79	21.55
T, °C	20	20
λ(Mo Kα), Å	0.709 26	0.709 26
monochromator	graphite	graphite
scan type	$\omega/2\theta$	$\omega/2\theta$
R^a	0.0374	0.0462
$R_w{}^b$	0.0432	0.0506

^{a} $R = \sum||F_o| - |F_c||/\sum|F_o|$. ^{b} $R_w = [\sum w||F_o| - |F_c||^2/\sum w|F_o|^2]^{1/2}$.

solutions range from 3.5 to 3.9, depending on the *x* value (x = 0, 0.35; x = 0.5, 3.7; x = 1, 3.9). By slow evaporation at ca. 35 °C, crystalline solids appeared after a few days. The solids were separated by vacuum filtration, washed with ethanol–water (1:2), and stored in a desiccator over silica gel. C, H, and N contents in the solids were determined by elemental analysis. Copper and nickel were determined by atomic absorption using a Perkin-Elmer 300 AA spectrophotometer. Analytical data are listed in Table I.

Physical Measurements. Diffuse-reflectance electronic spectra were recorded on a Pelkin-Elmer Lambda 9 UV/vis/near-IR spectrophotometer in the 7000–35 000-cm^{-1} range using the filter paper Nujol mull technique. Deconvolution of the experimental spectra were made using a modification of the Pitha and Jones program.[9]

Magnetic measurements were carried out on polycrystalline samples in the range 4–100 K with a pendulum-type apparatus equipped with a helium cryostat. Measurements from 4.2 to 1.8 K were made in a glass cryostat with pumped liquid helium. Experimental susceptibilities were corrected both for the diamagnetic contributions and the TIP of the Cu(II) ions, estimated to be 60×10^{-6} emu mol^{-1} per Cu(II) ion.[10]

Polycrystalline powder and single-crystal EPR spectra were recorded using Bruker ER-200 D (9.5 GHz) and Varian E15 (35 GHz) spectrometers equipped with a variable-temperature device.

Crystal Structure Determination of 1 and 2. The X-ray data were recorded with a CAD-4 Enraf-Nonius diffractometer. The intensities of four standard reflections were monitored throughout the data collection. No significant variation was detected. Lattice parameters were obtained by the centering of 24 reflections in the range $14 \le 2\theta \le 26$ for **1** and 25 reflections in the range $13 \le 2\theta \le 31$ for **2**. Lorentz and polarization corrections were applied. Absorption corrections were estimated to be unnecessary on the basis of small μ's. Other important features of data collection are summarized in Table II.

Data collection showed systematic absences (*h*00, *h* odd; 0*k*0, *k* odd; 00*l*, *l* odd; 0*kl*, *k* + *l* odd; *h*0*l*, *h* and *l* odd; *hk*0, *h* + *k* odd; *hkl*, *h* + *k* + *l* odd) which define two possible monoclinic space groups, *Ia* and *I*2/*a*.

The structure of **1** was solved by direct methods using the noncentrosymmetric space group *Ia* (Z = 4). The positions of the five metal atoms were determined using the program MULTAN 11/84.[11] The remaining non-hydrogen atoms were located from successive Fourier synthesis with the same program. Refinement of the structure was carried out with the SHELX-76 system[12] by isotropic full-matrix least-squares methods in a first stage. After refinement to R = 0.069, the space group was changed to *I*2/*a* since very large correlations were observed among the refined parameters. The five independent metal atoms per asymmetric unit in the noncentrosymmetric case were reduced to three, one of them occupying a special position (4*d*) in the space group *I*2/*a*. Anisotropic refinement of all non-hydrogen atoms yielded final values for R and R_w of 0.037 and 0.043. A total of 31 hydrogen atoms were located by difference Fourier maps and included at fixed positions in the refinement with common fixed isotropic thermal parameters (U = 0.05 Å^2). In the final difference map the residual maximum was a peak of 0.4 e Å^{-3} located near the nickel atom. Atomic scattering factors and corrections for anomalous dispersion for Cu and Ni atoms were taken from ref 13.

The structure of **2** was refined using the final parameters of **1** as starting data for all non-hydrogen atoms. Weighted anisotropic full-matrix least-squares methods for all non-hydrogen atoms with the SHELX-76 program gave final values of R and R_w of 0.0441 and 0.0496. The coordinates of the cdta's hydrogen atoms were calculated and included in the refinement at fixed positions with common fixed isotropic thermal parameters (U = 0.05 Å^2). The positions of nine hydrogen atoms belonging to water molecules were determined with use of difference Fourier maps and included in the refinement at fixed positions with common fixed isotropic thermal parameters (U = 0.05 Å^2). The residual maximum in the final difference map was one peak of density 0.95 e Å^{-3} located near one copper atom. The geometrical calculations were performed with XANADU.[14] The final atomic coordinates for **1** and **2** are given in Tables III and IV, respectively.

Results and Discussion

Synthesis. As it was previously reported,[8] the binuclear $Cu_2(cdta)\cdot 4H_2O$ and $CuNi(cdta)\cdot 7H_2O$ complexes are easily obtained as polycrystalline powders by addition of Me_2CO to aqueous solutions containing the appropriate metal nitrates and $cdta^{4-}$ in a 2:1 metal–$cdta^{4-}$ stoichiometric ratio. The subsequent storage of the solutions at ca. 5 °C leads to these powdered solids after several hours. In an effort to obtain suitable single crystals, the conditions of the synthesis were modified. So, the aqueous solutions containing the appropriate amounts of metallic ions and cdta were left to evaporate at ca. 35 °C without addition of any organic solvent. In both cases, well-formed blue prismatic crystals grew and, surprisingly, their X-ray diffraction patterns (which clearly show the isostructurality of both new solids) turned out different from those previously found for 3d-bimetallic complexes in the cdta family.[4,5,6b,d] When the C, N, and metal contents of these new products were determined, a 2.5:1 metal–cdta ratio was found. Obviously, the seeming excess of positive charge implied by this ratio requires the presence in the solids of an anion other than cdta. Because of the synthetic procedure, the only possible counterion is nitrate. In fact the presence of NO_3^- groups was confirmed by qualitative analysis and IR spectroscopy. This, and the analytical data, allowed us to propose $Cu_3M_2(cdta)_2(NO_3)_2\cdot 15H_2O$ (M = Cu, Ni) as the empirical formula for these new cdta derivatives. On the other hand, both novel compounds can be reproducibly obtained starting from aqueous solutions containing the metal nitrates and cdta in the stoichiometric relationships (see Experimental Section).

Crystal Structure of $Cu_3[Ni_2(cdta)]_2(NO_3)_2\cdot 15H_2O$ (1) and $Cu_3[Cu_2(cdta)]_2(NO_3)_2\cdot 15H_2O$ (2). Figure 1 shows a projection of the structure along [001]. Figure 2 shows the coordination geometries. Selected bond distances and angles are listed in Tables V and VI. The two most relevant features of this new structural type in the cdta family include the existence of three different classes of coordination sites and the resulting connection pattern among them. Thus, M(3) (M = Cu, Ni) atoms occupy a

(9) Pitha, J.; Jones, R. N. Program PC-116. National Council of Canada, Ottawa, 1967.
(10) Earnshaw, A. In *Introduction to Magnetochemistry*; Academic Press: London and New York, 1968.
(11) Main, P.; Germain, G.; Woolfson, M. M. MULTAN 11/84, System of Computer Programs for the Automatic Solution of Crystal Structures from X-Ray Diffraction Data. University of York (England) and Louvain (Belgium), 1984.
(12) Sheldrick, G. M. Program for Crystal Structure Determination. University of Cambridge, 1976.
(13) *International Tables for X-Ray Crystallography*; Kynoch Press: Birmingham, England, 1974; Vol. 1, pp 72, 99.
(14) Roberts, P.; Sheldrich, G. M. XANADU, Program for Crystallographic Calculations. University of Cambridge, 1975.

Table III. Positional Parameters and Their Estimated Standard Deviations (in Parentheses) for Compound **1**

	x	y	z	B_{eq},[a] Å^2
Ni(3)	0.68693 (2)	0.04679 (6)	0.39145 (2)	1.95 (1)
Cu(1)	0.88136 (2)	0.32223 (6)	0.47053 (2)	2.33 (1)
Cu(2)	0.75000	−0.25000	0.25000	2.64 (2)
N(1)	0.4009 (2)	−0.0970 (5)	0.8274 (1)	3.8 (1)
N(10)	0.5931 (1)	0.0415 (4)	0.3743 (1)	2.06 (8)
N(20)	0.6943 (1)	0.2604 (4)	0.3529 (1)	2.00 (7)
O(W1)	0.9583 (2)	0.4561 (5)	0.4333 (1)	4.07 (9)
O(W2)	0.8610 (1)	0.5359 (4)	0.5025 (1)	3.12 (8)
O(W3)	0.8924 (1)	0.0949 (4)	0.4440 (1)	3.27 (8)
O(W4)	0.8352 (2)	−0.2722 (4)	0.2700 (1)	4.0 (1)
O(W5)	0.0591 (1)	0.1549 (4)	0.5069 (1)	3.96 (9)
O(W6)	0.3706 (2)	0.0503 (5)	0.3309 (1)	5.6 (1)
O(W7)	0.3190 (2)	0.2230 (6)	0.4074 (2)	7.2 (2)
O(W8)	0.2500	0.2191 (9)	0.0000	6.6 (2)
O(N9)	0.4080 (2)	0.0385 (5)	0.8484 (1)	5.8 (1)
O(N10)	0.3701 (2)	−0.0987 (5)	0.7926 (1)	5.3 (1)
O(N11)	0.4264 (2)	−0.2292 (5)	0.8409 (2)	6.0 (1)
O(11)	0.6679 (1)	−0.1827 (4)	0.4177 (1)	2.77 (7)
O(12)	0.5944 (1)	−0.3844 (4)	0.4164 (1)	2.97 (7)
O(21)	0.7737 (1)	0.1350 (4)	0.4124 (1)	2.60 (7)
O(22)	0.8171 (1)	0.3910 (4)	0.4275 (1)	2.67 (6)
O(31)	0.6532 (1)	0.1764 (4)	0.4475 (1)	2.96 (8)
O(32)	0.5645 (1)	0.2504 (4)	0.4804 (1)	2.66 (7)
O(41)	0.7168 (1)	−0.0800 (4)	0.3330 (1)	2.98 (7)
O(42)	0.7507 (1)	−0.0124 (4)	0.2653 (1)	3.02 (7)
C(10)	0.5898 (2)	0.1476 (5)	0.3325 (1)	2.02 (9)
C(11)	0.5807 (2)	−0.1446 (5)	0.3684 (1)	2.5 (1)
C(12)	0.6163 (2)	−0.2451 (5)	0.4038 (1)	2.5 (1)
C(20)	0.6287 (2)	0.3115 (5)	0.3409 (1)	2.02 (9)
C(21)	0.7275 (2)	0.3894 (5)	0.3807 (1)	2.30 (9)
C(22)	0.7763 (2)	0.2958 (5)	0.4092 (1)	2.3 (1)
C(30)	0.6237 (2)	0.4386 (5)	0.3030 (2)	3.0 (1)
C(31)	0.5566 (2)	0.1093 (6)	0.4115 (1)	2.5 (1)
C(32)	0.5955 (2)	0.1826 (5)	0.4487 (1)	2.31 (9)
C(40)	0.5553 (2)	0.4788 (6)	0.2919 (2)	3.3 (1)
C(41)	0.7345 (2)	0.2149 (5)	0.3150 (1)	2.4 (1)
C(42)	0.7328 (2)	0.0252 (5)	0.3040 (1)	2.4 (1)
C(50)	0.5220 (2)	0.3160 (6)	0.2786 (1)	3.0 (1)
C(60)	0.5237 (2)	0.1858 (5)	0.3166 (1)	2.8 (1)

[a] $B_{eq} = 8\pi^2[(U_{11} + U_{22} + U_{33})/3]$.

Table IV. Positional Parameters and Their Estimated Standard Deviations (in Parentheses) for Compound **2**

	x	y	z	B_{eq},[a] Å^2
Cu(3)	0.68905 (3)	0.04723 (10)	0.39046 (3)	2.23 (2)
Cu(1)	0.88228 (4)	0.32253 (10)	0.47036 (3)	2.39 (2)
Cu(2)	0.75000	−0.25000	−0.25000	2.56 (2)
N(1)	0.4037 (3)	−0.0959 (9)	0.8296 (2)	4.0 (2)
N(10)	0.5947 (2)	0.0461 (7)	0.3757 (2)	2.1 (1)
N(20)	0.6964 (2)	0.2567 (6)	0.3523 (2)	2.0 (1)
O(W1)	0.9603 (2)	0.4535 (7)	0.4341 (2)	4.3 (1)
O(W2)	0.8603 (2)	0.5417 (6)	0.5007 (2)	3.1 (1)
O(W3)	0.8942 (2)	0.0936 (6)	0.4452 (2)	3.6 (1)
O(W4)	0.8356 (2)	−0.2724 (7)	0.2721 (2)	4.0 (1)
O(W5)	0.0570 (2)	0.1585 (6)	0.5062 (2)	4.2 (1)
O(W6)	0.3697 (3)	0.0441 (8)	0.3319 (2)	5.5 (2)
O(W7)	0.3257 (4)	0.2260 (9)	0.4071 (3)	7.7 (2)
O(W8)	0.2500	0.212 (2)	0.0000	7.5 (3)
O(N9)	0.4105 (3)	0.0383 (9)	0.8500 (2)	6.1 (2)
O(N10)	0.3715 (3)	−0.1003 (8)	0.7960 (2)	5.7 (2)
O(N11)	0.4302 (3)	−0.2294 (8)	0.8425 (2)	6.4 (2)
O(11)	0.6724 (2)	−0.1765 (6)	0.4175 (2)	2.8 (1)
O(12)	0.6006 (2)	−0.3855 (6)	0.4176 (2)	3.0 (1)
O(21)	0.7750 (2)	0.1326 (6)	0.4119 (2)	2.7 (1)
O(22)	0.8194 (2)	0.3901 (6)	0.4268 (1)	2.83 (9)
O(31)	0.6541 (2)	0.1918 (7)	0.4494 (2)	3.3 (1)
O(32)	0.5641 (2)	0.2549 (6)	0.4803 (1)	2.6 (1)
O(41)	0.7158 (2)	−0.0903 (6)	0.3282 (1)	3.0 (1)
O(42)	0.7512 (2)	−0.0079 (6)	0.2637 (1)	2.9 (1)
C(10)	0.5908 (3)	0.1479 (8)	0.3340 (2)	2.2 (1)
C(11)	0.5831 (3)	−0.1438 (8)	0.3710 (2)	2.6 (1)
C(12)	0.6207 (3)	−0.2425 (9)	0.4045 (2)	2.7 (1)
C(20)	0.6307 (3)	0.3115 (8)	0.3405 (2)	1.9 (1)
C(21)	0.7303 (3)	0.3875 (8)	0.3796 (2)	2.4 (1)
C(22)	0.7786 (3)	0.2931 (8)	0.4079 (2)	2.3 (1)
C(30)	0.6259 (3)	0.4335 (9)	0.3014 (2)	2.9 (2)
C(31)	0.5585 (3)	0.1189 (9)	0.4112 (2)	2.6 (2)
C(32)	0.5963 (3)	0.1930 (9)	0.4498 (2)	2.4 (1)
C(40)	0.5568 (3)	0.476 (1)	0.2906 (3)	3.7 (2)
C(41)	0.7377 (3)	0.2116 (8)	0.3148 (2)	2.4 (1)
C(42)	0.7333 (3)	0.0222 (8)	0.3021 (2)	2.4 (1)
C(50)	0.5225 (3)	0.312 (1)	0.2797 (2)	3.2 (2)
C(60)	0.5243 (3)	0.1863 (9)	0.3181 (2)	2.7 (1)

[a] $B_{eq} = 8\pi^2[(U_{11} + U_{22} + U_{33})/3]$.

"chelated" position defined by two nitrogen and four oxygen atoms belonging to a cdta group which acts as a sexidentate ligand. Moreover, the structure involves two different cationic "hydrated" positions occupied by copper atoms. The copper environments are either square-pyramidal or square-planar. In the former, the Cu(II) ions are bound to two water molecules and two oxygen atoms belonging to carboxylate groups from two different $[M(3)cdta]^{2-}$ entities. The apical ligand is another water molecule. On the other hand, copper atoms in square-planar positions lie on symmetry centers (*4d* sites). They are bound to two water molecules and two oxygen atoms from different anionic $[M(3)cdta]^{2-}$ units. This way, there are three different carboxylate bridging groups connecting the metallic centers. The resulting infinite chains are constituted from rings, made up of pairs of $[M(cdta)]^{2-}$ and five-coordinate coppers, alternating with four-coordinate coppers. These ...$[O_{III}Cu(OH_2)_2O_{III}]$...{[M(cdta)]...$[O_ICu(OH_2)_3O_{II}]_2$...[M(cdta)]}... chains run parallel to the [001] axis.

The crystal packing is due to hydrogen bonding between water molecules and carboxylate groups, whereas the nitrate ions, linked (through hydrogen bonds) to only one chain, do not contribute significantly to *interchain* connections.

The coordination polyhedron around the M(3) atom is a distorted octahedron. The basal plane is comprised of the two nitrogen atoms and two oxygen atoms [O(11), O(21)] from type G carboxylates.[15] The M–N and M–O bond distances (M(3)–N(av) = 2.06 (2) and 2.04 (4) Å, M(3)–O_G(av) = 2.04 (5) and 2.00 (7) Å for **1** and **2**, respectively) are similar to those previously reported for edta and cdta bimetallates containing nickel or copper atoms in the chelated positions. The axial sites are occupied by oxygen atoms belonging to type R carboxylates with M(3)–O_R average distances of 2.11 (2) Å for **1** and 2.268 (9) Å for **2**. The tetragonality *T* (defined as the mean in-plane M(3)–O,N bond length divided by the mean out-of-plane M(3)–O bond length)[16a,d] is 0.97 and 0.89 for **1** and **2**, respectively. Thus, as might be expected, the distortion is much more pronounced when the copper atoms are occupying this position. The coordination of Cu(3) may then be viewed as 4 + 2, which agrees with Jahn–Teller active six-coordinate copper(II) complexes.[16]

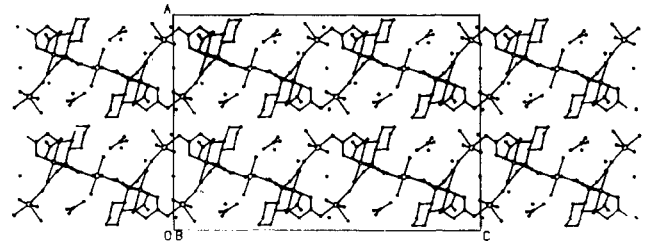

Figure 1. Projection of the structure along [001] showing the contents of the unit cell.

(15) Weakliem, H. A.; Hoard, J. L. *J. Am. Chem. Soc.* **1959**, *81*, 549.

(16) (a) Hathaway, B. J.; Billing, D. E. *Coord. Chem. Rev.* **1970**, *5*, 143. (b) Hathaway, B. J.; Duggan, M.; Murphy, A.; Mullone, J.; Power, C. P.; Walsh, A.; Walsh, B. *Coord. Chem. Rev.* **1981**, *36*, 267. (c) Hathway, B. J. *Coord. Chem. Rev.* **1983**, *52*, 87. (d) Hathaway, B. J. In *Comprehensive Coordination Chemistry*; Wilkinson, G., Gillard, R. D., McCleverty, F., Eds.; Pergamon Press: Oxford, England, 1985; Vol. 5, p 601.

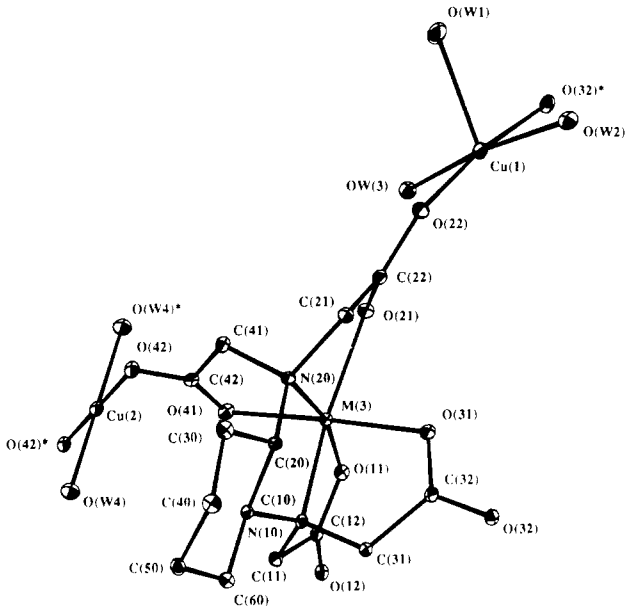

Figure 2. Perspective view and atomic numbering scheme of $Cu_3[M(3)(cdta)]_2(NO_3)_2 \cdot 15H_2O$ [M(3) = Ni in **1** and M = Cu in **2**]. O(32)* is obtained from O(32) (through the symmetry operation $^3/_2 - x, y, 1 - z$) and O(42)* and O(W4)* from O(42) and O(W4)* (through the symmetry operation $^3/_2 - x, ^1/_2 - y, ^1/_2 - z$), respectively. Nitrate anions and lattice water molecules were omitted for clarity.

Table V. Selected Bond Distances (Å) Found in Compounds **1** and **2**

	1	2
	Coordination Polyhedra	
N(10)–M(3)	2.072 (3)	2.062 (5)
N(20)–M(3)	2.039 (3)	2.008 (5)
O(11)–M(3)	2.001 (3)	1.956 (4)
O(21)–M(3)	2.077 (3)	2.053 (4)
O(31)–M(3)	2.101 (3)	2.266 (5)
O(41)–M(3)	2.124 (3)	2.270 (4)
O(W1)–Cu(1)	2.257 (3)	2.263 (5)
O(W2)–Cu(1)	1.977 (3)	1.996 (5)
O(W3)–Cu(1)	1.961 (3)	1.952 (5)
O(22)–Cu(1)	1.962 (3)	1.953 (4)
O(32*)–Cu(1)	1.956 (3)	1.957 (4)
O(W4)–Cu(2)	1.925 (3)	1.951 (5)
O(42)–Cu(2)	1.911 (3)	1.921 (4)
	Carboxylate Groups	
C(12)–O(11)	1.277 (5)	1.276 (8)
C(12)–O(12)	1.245 (5)	1.256 (8)
C(22)–O(21)	1.260 (5)	1.251 (8)
C(22)–O(22)	1.270 (5)	1.282 (7)
C(32)–O(31)	1.239 (5)	1.237 (8)
C(32)–O(32)	1.282 (5)	1.266 (8)
C(42)–O(41)	1.249 (5)	1.246 (8)
C(42)–O(42)	1.267 (5)	1.268 (8)

The cdta conformation is E,G/R.[17] The angles and bond distances in the ligand are in agreement with those found in other cdta complexes with low angular strain in the rings.[4,5,6b,d]

The unique unidentate carboxylate group is asymmetric, with C–O bond distances satisfying the relation C(12)–O(11) > C(12)–O(22) (1.277 (5) and 1.245 (5) Å for **1** and 1.276 (8) and 1.256 (8) Å for **2**), as expected from the polarization of the charge density toward the metal-bonded oxygen atom. The bridging carboxylate groups are less asymmetric and, in this case, the C–O distances satisfy the relation C(*n*2)–O(*n*1) < C(*n*2)–O(*n*2) (i.e., the polarization of the charge density in the bridging carboxylates takes place toward the oxygen atom more strongly bonded to the metal). The structural formation of the COO groups is *a*-2-*s* (anti–syn)[18] for all three different bridging carboxylates.

Table VI. Selected Bond Angles (deg) of Coordination Polyhedra Found in Compounds **1** and **2**

	1	2
N(20)–M(3)–N(10)	87.2 (1)	87.8 (2)
O(11)–M(3)–N(10)	83.2 (1)	84.5 (2)
O(11)–M(3)–N(20)	166.9 (1)	168.3 (2)
O(21)–M(3)–N(10)	161.3 (1)	160.2 (2)
O(21)–M(3)–N(20)	80.2 (1)	81.3 (2)
O(21)–M(3)–O(11)	111.1 (1)	108.5 (2)
O(31)–M(3)–N(10)	82.7 (1)	80.9 (2)
O(31)–M(3)–N(20)	95.3 (1)	95.6 (2)
O(31)–M(3)–O(11)	92.4 (1)	91.9 (2)
O(31)–M(3)–O(21)	84.7 (1)	83.7 (2)
O(41)–M(3)–N(10)	94.5 (1)	94.2 (2)
O(41)–M(3)–N(20)	83.3 (1)	82.2 (2)
O(41)–M(3)–O(11)	88.5 (1)	89.6 (2)
O(41)–M(3)–O(21)	97.7 (1)	100.6 (2)
O(41)–M(3)–O(31)	177.0 (1)	174.7 (2)
O(W2)–Cu(1)–O(W1)	90.9 (1)	91.7 (2)
O(W3)–Cu(1)–O(W1)	97.2 (1)	96.3 (2)
O(W3)–Cu(1)–O(W2)	171.8 (1)	172.0 (2)
O(22)–Cu(1)–O(W1)	93.2 (1)	92.8 (2)
O(22)–Cu(1)–O(W2)	86.3 (1)	85.8 (2)
O(22)–Cu(1)–O(W3)	93.6 (1)	93.7 (2)
O(32*)–Cu(1)–O(W1)	94.4 (1)	94.2 (2)
O(32*)–Cu(1)–O(W2)	90.3 (1)	90.3 (2)
O(32*)–Cu(1)–O(W3)	88.7 (1)	89.1 (2)
O(32*)–Cu(1)–O(22)	171.7 (1)	172.2 (2)
O(42)–Cu(2)–O(W4)	90.4 (1)	90.1 (2)

The coordination polyhedron around Cu(1) is a square pyramid. The basal plane is formed by two water molecules (O(W2) and O(W3)) and two trans-oxygen atoms belonging to one R and one G carboxylate group (O(22), O(32)) from different chelated entities. The four atoms are practically coplanar with deviations from the mean planes lower than ±0.008 and ±0.009 Å for **1** and **2**, respectively. The copper–oxygen bond distances are normal, with average values of 1.96 (2) Å for **1** and 1.96 (2) Å for **2**. The apex of the pyramid is occupied by an oxygen atom of a water molecule, with bond distances of 2.257 (3) Å for **1** and 2.263 (5) Å for **2**. As expected, the copper atom is displaced (0.13 Å for both compounds) from the basal plane toward the apex, the tetragonality parameter (*T*) obtained in both cases being 0.87. The distortion of the CuO_5 polyhedron can be quantified by using the approach of Muetterties and Guggenberger.[19] The key shape-determinant dihedral angle, e_3 (O(22)–O(W3)–O(32*)–O(W2)) is 0.0° for an ideal square pyramid (SPY) and 53.1° for an ideal trigonal bipyramid (TBP). For both compounds e_3 is 1.0°, indicating an absolute predominance of the SPY form.

The coordination polyhedron geometry around Cu(2) is square-planar. The metal atom is bound to two water molecules, O(W4) and O(W4*), and two oxygen atoms belonging to R carboxylate groups from different chelated entities, O(42) and O(42*). The copper–oxygen bond distances are normal, average 1.92 (1) Å for **1** and 1.94 (2) Å for **2**, the deviations from the mean plane being less than ±0.001 Å.

It must be finally stressed that the existence of the three coordination environments (one chelated and two different hydrated) is a feature which, a priori, makes this structure especially versatile to be used as a host lattice for the stabilization of new ordered low-dimensional systems.

Occupational Ordering. As suggested above, dealing with this kind of bimetalate, a key question concerning the desired properties refers to the possibility of inducing a given metallic atom sequence on the basis of the selective occupation of the coordination sites. In this sense, as discussed earlier,[4a] the inertness of the $[Ni(cdta)]^{2-}$

(17) Porai-Koshits, M. A.; Pozhidaev, A. I.; Polynova, T. N. *Zh. Struk. Khim.* **1974**, *15*, 1117.

(18) Porai-Koshits, M. A. *Zh. Struk. Khim.* **1980**, *21*, 146.

(19) Muetterties, E. L.; Guggenberger, L. J. *J. Am. Chem. Soc.* **1974**, *96*, 1748.

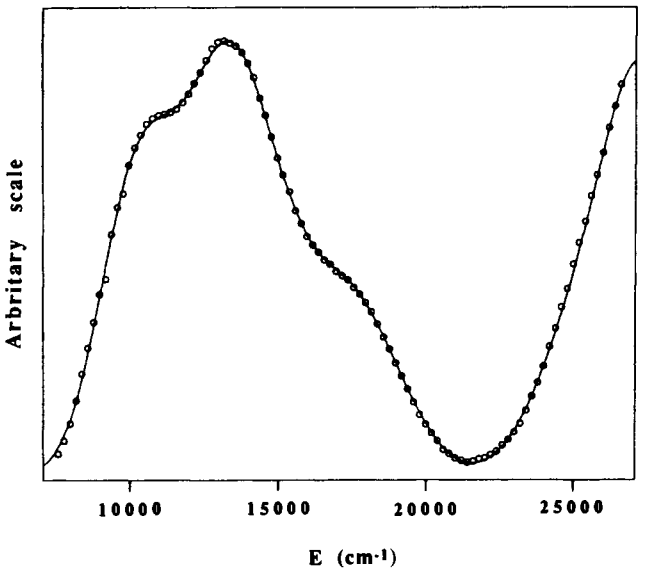

Figure 3. Comparative analysis of the experimental (O) and deconvoluted (—) spectra of the $[Cu_3,Ni_2]$ complex.

Table VII. Visible Spectral Analysis of $[Cu_3Ni_2]$: Experimental Energies (cm^{-1}) and Assigned Transitions

$[CuO_4]$ chromophore	$[CuO_5]$ chromophore	$[NiN_2O_4]$ chromophore
18 520 (^2E_g, $^2A_{2g} \leftarrow {}^2B_{1g}$)	13 170 ($^2E \leftarrow {}^2B_1$)	27 480 ($^3T_{1g}(P) \leftarrow {}^3A_{2g}$)
15 150 ($^2B_{2g} \leftarrow {}^2B_{1g}$)	9 930 ($^2B_2 \leftarrow {}^2B_1$)	25 300 ($^1T_{1g} \leftarrow {}^3A_{2g}$)
	8 870 ($^2A_1 \leftarrow {}^2B_1$)	16 960 ($^3T_{1g}(F) \leftarrow {}^3A_{2g}$)
		13 175 ($^1E_g \leftarrow {}^3A_{2g}$)
		10 430 ($^3T_{2g} \leftarrow {}^3A_{2g}$)

complex in solution makes it of particular interest for the synthesis of ordered bimetallic derivatives by introducing a kinetic factor which may overcome thermodynamic restrictions.

Accordingly, taking into account that the synthesis of compound **1** (hereinafter $[Cu_3,Ni_2]$) occurs under kinetic control conditions, it can be expected that the chelated position in this system is occupied by the nickel(II) ion. From this idea, we have devised a set of experiments intended to establish the existence of a limit for the nickel(II) substitution in the structure. Thus, we prepared a set of solutions containing a 2.5:1 metal–cdta molar ratio in such a way that the Ni/M (M = Cu + Ni) relation ranged from 0 to 1.

All the solids isolated from solutions having Ni/M < 0.4 ratios were isostructural to the compound **2** (hereinafter $[Cu_3,Cu_2]$). The analytical data showed that the Ni and Cu contents in the solids were the same, within the experimental error, as those in the starting solution. On the contrary, when the Ni/M ratio in the starting solution was higher than 0.4, the crystalline phase $[Cu_3,Ni_2]$ resulted. Clearly, these results indicate that the nickel(II) ions are able to replace only the copper(II) ones occupying the chelated positions. So, the existence of a "solid solution" of composition $Cu_3[Cu_{1-x}Ni_x(cdta)]_2(NO_3)_2 \cdot 15H_2O$ may be stated, where the $[Cu_3,Cu_2]$ and $[Cu_3,Ni_2]$ derivatives may be considered as the "pure limit compounds".

Accordingly, deviations from regular geometry of the octahedral environment of the chelated positions may help to identify the nickel atom locations. As the structural data show, axial distortions are significantly more pronounced in $[Cu_3,Cu_2]$ than in $[Cu_3,Ni_2]$, which clearly supports the occupational preference of Ni(II) ions for this position.

The occupational ordering was again confirmed by visible spectroscopy. This conclusive method has already been successfully used for several edta and cdta derivatives.[4a,8] Assuming the same basic hypothesis detailed in ref 8, the experimental diffuse-reflectance spectrum of $[Cu_3,Ni_2]$ (Figure 3) is reasonably well interpreted in terms of CuO_4 (D_{4h}), CuO_5 (C_{4v}) and NiN_2O_4

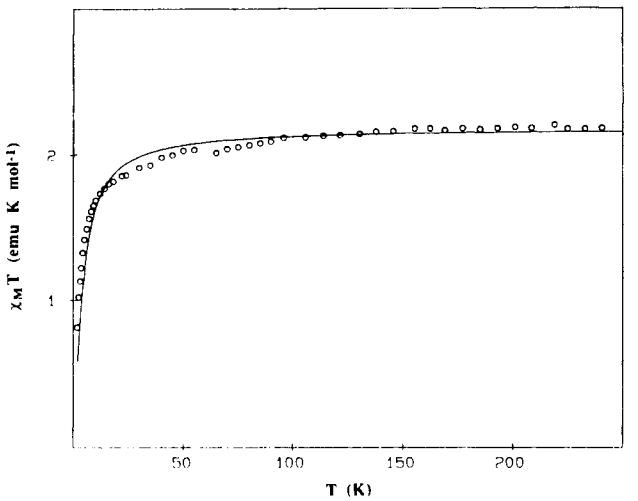

Figure 4. Magnetic behavior of the $[Cu_3,Cu_2]$ compound.

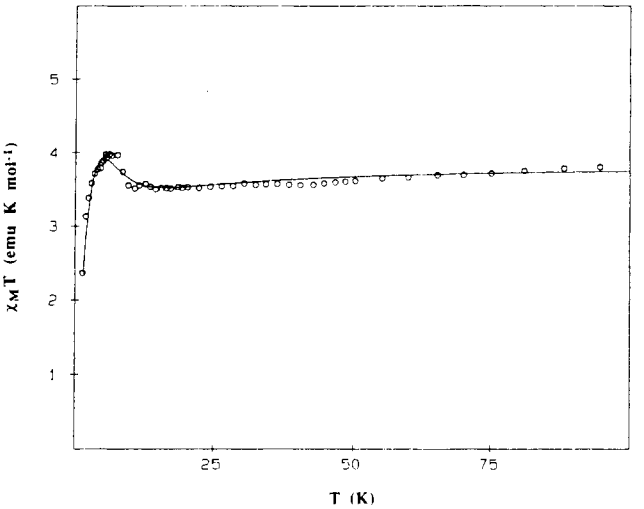

Figure 5. Magnetic behavior of the $[Cu_3,Ni_2]$ compound.

(C_{2v}) chromophores. The experimental energies and the assigned transitions are listed in Table VII. As expected, the set of crystal field parameters obtained for the NiN_2O_4 chromophore (Dq = 1043 cm^{-1}, B' = 860 cm^{-1}) is similar to those previously reported for other related edta and cdta derivatives.[8]

Magnetic Properties. The magnetic behavior of $[Cu_3,Cu_2]$ is illustrated in the Figure 4 by means of a plot of $\chi_M T$ vs T in the range 1.8–250 K. $\chi_M T$ is nearly temperature independent between 250 and 20 K, with a value close to 2 emu·K·mol^{-1}, which, in turn, is close to the expected value for five uncoupled $^1/_2$ spins. It shows a decrease at $T < 20$ K, in agreement with the preeminence of antiferromagnetic interactions between the copper(II) ions. On the other hand the magnetic behavior of $[Cu_3,Ni_2]$ is displayed in Figure 5. The $\chi_M T$ product decreases slightly upon cooling, reaching a minimum at $T = 15$ K. Then, $\chi_M T$ increases abruptly until it reaches a maximum at $T = 7$ K and finally goes down suddenly.

In view of the structure, both compounds may be considered as one-dimensional systems involving three magnetic sublattices schematized as follows:

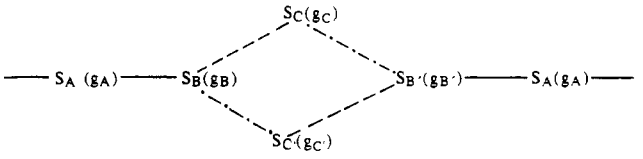

Here $S_A = S_C = {}^1/_2$, while $S_B = {}^1/_2$ for $[Cu_3,Cu_2]$ and 1 for $[Cu_3,Ni_2]$. g_A, g_B, and g_C are the Landé factors related to the

three types of interacting ions, on sites A (square planar) B, B′ (octahedral), and C, C′ (square pyramidal). On the basis of symmetry considerations, the B, B′ and C, C′ sites are equivalent as well as the B–C, B′–C′ and B–C′, B′–C exchange interactions. Thus, if we represent by J_{ij} the exchange constant between the magnetic moments on sites i and j, we state the following set of relations:

$$J_{AB} = J \qquad J_{BC} = J_{B'C'} = J_1 \qquad J_{B'C} = J_{BC'} = J_2$$

$$g_A = g_1 \qquad g_B = g_{B'} = g_2 \qquad g_C = g_{C'} = g_3$$

Further, we will assume in a first step that only the z components of the spins are coupled and that the external magnetic field is applied along the quantization axis. Bearing this consideration in mind, exact expressions of the zero-field parallel magnetic susceptibility ($\chi_\parallel$) can be obtained using the transfer matrix procedure.[20] This one consists of determining the transfer matrix (T) which relates the partition functions Z_N and Z_{N+1} when a repeat unit (Cu_3,Cu_2) or (Cu_3,Ni_2) is added to a semiinfinite chain. Basically, we must solve a square matrix of size 32×32 ([Cu_3Cu_2]) or 72×72 ([Cu_3Ni_2]). In fact, it appears that the transfer matrix (T) results from the appropriate product of four matrices and that it reduces to 2×2 for the copper and copper–nickel chains. In the limit of very long chains, the partition function is related to the largest eigenvalue U_+ of (T). The zero-field magnetic susceptibility is then easily derived from the second derivative of log (U_+) with respect to the field. Further, this procedure allows one to take into account a uniaxial anisotropy along the quantization axis for the Ni(II) ion. Clearly, the nature of the ions involved in these compounds would make more appropriate an isotropic exchange Hamiltonian but, in this case, only numerical solutions for the susceptibility are available. So, the choice of an anisotropic interaction, even if this is questionable, allows an analytical treatment of this problem retaining all the features of this complex one-dimensional system.

For the copper chain, the Hamiltonian can be written as

$$\hat{H} = \hat{H}_{ex} + \hat{H}_{Zee} = \sum_i (-J\hat{S}^z_{Ai}\hat{S}^z_{Bi} - J_1\hat{S}^z_{Bi}\hat{S}^z_{Ci} - J_2\hat{S}^z_{Bi}\hat{S}^z_{C'i} - J_2\hat{S}^z_{Ci}\hat{S}^z_{B'i} - J_1\hat{S}^z_{C'i}\hat{S}^z_{B'i} - J\hat{S}^z_{B'i}\hat{S}^z_{Ai} - g_1\mu_B H\hat{S}^z_{Ai} - g_2\mu_B H(\hat{S}^z_{Bi} + \hat{S}^z_{B'i}) - g_3\mu_B H(\hat{S}^z_{Ci} + \hat{S}^z_{C'i}))$$

where μ_B is the Bohr magneton and H the applied magnetic field.

Clearly, for antiferromagnetic interactions, each elementary unit (Cu_3Cu_2) exhibits an uncompensated spin $S = {}^1/_2$ so that 1-D ferromagnetism should be observed. In the title compound there is no significant difference between the Landé factors for copper(II) ions in different sites ($\Delta g < 0.2$), and we have considered single g parameter for [Cu_3,Cu_2]. In this assumption, the experimental data can be satisfactorily fitted according the set of parameters $g = 2.14$, $J/k = -1$ K, $J_1/k = -12$ K, and $J_2/k = -1$ K (Figure 4). Obviously, for symmetry reasons, the J_1 and J_2 values may be interchanged. It thus appears that the two equivalent exchange pathways named B–C and B′–C′ (or alternatively B′–C and B–C′, since a priori both possibilities are indistinguishable) are negligible. In the same way, the exchange coupling between the A and B sites is weak and negative.

Considering now that the Heisenberg model is more appropriate for interacting copper(II) ions, we have assumed in a second step isotropic couplings within the 1-D system. Due to the memory size of the computer available, the calculations were limited to two elementary units (Cu_3Cu_2) with a connection between outer copper(II) ions to avoid boundary effects. Owing to the limited number of spins, such a treatment gives only, as the previous one, approximate values of the exchange constants. The spin Hamiltonian was solved numerically by diagonalizing the block matrices built up in the subspaces $|S^z_A S^z_B S^z_C ...\rangle$, characterized by a given value of the z component of the total spin quantum number $S^z = \sum_i S^z_i$. The best fitting parameters corresponds to $J/k = 0$ K and $J_1/k = -12$ K whereas J_2/k shows a variability, ranging between −1 and −6 K, related to the poor sensitivity of the fitting procedure. These values are in good accordance with those obtained with the anisotropic model. Although all these models must be thought of as questionable, the results appear to be available for describing the behavior of the [Cu_3,Cu_2] compound in the temperature range of interest.

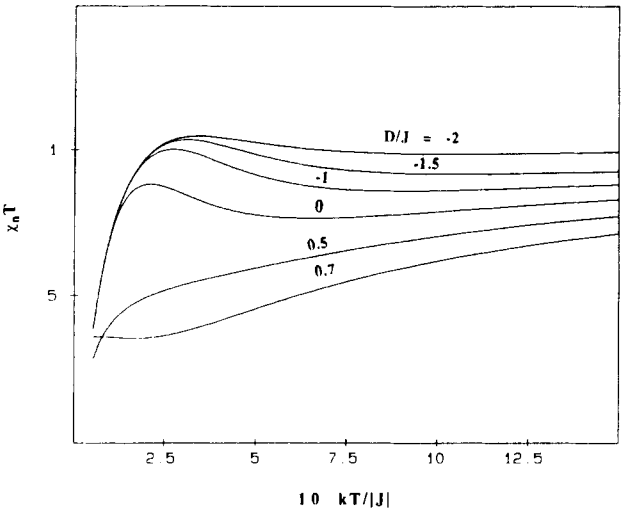

Figure 6. Influence of the D/J ratio on the theoretical magnetic behavior derived from the proposed model for the [Cu_3,Ni_2] system (see text).

With regard to the [Cu_3,Ni_2] compound, made of alternating copper(II) and nickel(II) ions, the overall Hamiltonian is given by

$$\hat{H} = \sum_i (-J\hat{S}^z_{Ai}\hat{S}^z_{Bi} - J_1\hat{S}^z_{Bi}\hat{S}^z_{Ci} - J_2\hat{S}^z_{Bi}\hat{S}^z_{C'i} - J_2\hat{S}^z_{Ci}\hat{S}^z_{B'i} - J_1\hat{S}^z_{C'i}\hat{S}^z_{B'i} - J\hat{S}^z_{B'i}\hat{S}^z_{Ai} - g_1\mu_B H\hat{S}^z_{Ai} - g_2\mu_B H(\hat{S}^z_{Bi} + \hat{S}^z_{B'i}) - g_3\mu_B H(\hat{S}^z_{Ci} + \hat{S}^z_{C'i}) - D((\hat{S}^z_{Bi})^2 + (\hat{S}^z_{B'i})^2))$$

where D is the anisotropy constant (zero-field splitting) of spins on sites B and B′ with $S_{Ai} = S_{Ci} = S_{C'i} = {}^1/_2$ and $S_{Bi} = S_{B'i} = 1$.

In order to reproduce the experimental behavior of the [Cu_3,Ni_2] compound, we have studied the temperature dependence of χT for various combinations of the exchange and local distorsion parameters. Clearly, two limiting situations may be encountered depending on the anisotropy constant D:

1. For a negative and large D value (compared to the exchange constants), the singlet $S_z = 0$ is stabilized with respect to $S_z = \pm 1$ for each nickel(II) ion. Accordingly, the copper(II) ions feel no exchange field to first order and may be considered as isolated. The χT value is nearly independent of temperature.

2. For a positive and large value D value, the ground state of each nickel(II) ion is the doublet $S_z = \pm 1$. Owing to the splitting of this one when an external field is applied, one can assume that only $S = {}^1/_2$ spins are involved with alternating Landé factors. A ferrimagnetic-like behavior is expected like in the case of the copper(II) chain.

Finally, intermediate behaviors close to that observed experimentally occur when considering negative values of the exchange constants and a D/J ratio with negative values or slightly positive ones. In Figure 6, we have plotted the theoretical variation of $\chi_n T$ versus kT/J for some significant values of D/J, with $J < 0$,

(20) Kramers, H. A.; Wannier, C. H. *Phys. Rev.* **1941**, *60*, 252.

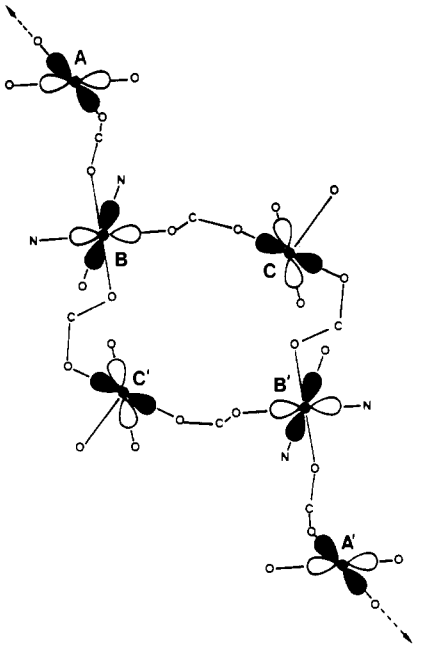

Figure 7. Relative orientation of the copper $d_{x^2-y^2}$ orbitals in the $[Cu_3,Cu_2]$ system.

$J'/J = 0.1$ ($J' = J_1 + J_2$), and $J_1/J_2 = 0$, χ_n being the normalized susceptibility:

$$\chi_n = \frac{\chi}{\frac{N\beta^2}{3k_B}(3/4(g_1^2 + 2g_3^2) + 4g_2^2)}$$

Assuming the same g value for the copper(II) ions (i.e., the g value obtained for the $[Cu_3,Cu_2]$ compound, $g = 2.14$), the best fit of the experimental data with the proposed model is obtained for $g_2 = 2.25$, $J/k = -15$ K, $J_2/k = -2$ K, and $D/k = 15$ K, with J_1 set to zero. When this parameter is let free to vary, we observe a divergence of the $\chi_n T$ product, which disagrees with the experimental data.

Magnetostructural Correlations. The relative orientation of the coordination polyhedra with regard to the bridging groups is responsible for the σ-bonding orientation of the magnetic orbitals (i.e., the spin-carrying orbitals). Moreover, the nature of the bridging groups is also the determinant for the intensity of the interaction. As it is well-known, bridging carboxylate groups provide usually poor support for the propagation of the exchange, leading to relatively weak interactions (except when the structural function is *s*-2-*s*[21]). In the new cdta structural type here reported, the bridging COO groups are *a*-2-*s*, and consequently, one may expect relatively weak interactions, regardless the magnetic orbital orientations.

In the $[Cu_3,Cu_2]$ compound, the magnetic orbitals containing the unpaired electrons are built up from the $d_{x^2-y^2}$ metallic orbital lying in the equatorial plane of the coordination polyhedra. As displayed in Figure 7, the copper polyhedra are connected in such a way that the overlap between the magnetic orbitals is efficient for Cu(1)–Cu(3), only. Thus, it can be stated that J_1 parameter (i.e., the strongest interaction) corresponds to the equivalent B–C and B′–C′ pathways.

A discussion of the experimental behavior of the $[Cu_3,Ni_2]$ compound needs to introduce the influence of competing effects, namely the antiferromagnetic interactions between magnetic moments and the zero-field splitting for nickel(II) ions. The two unpaired electrons of the Ni(II) ions occupy $d_{x^2-y^2}$ and d_{z^2} orbitals pointing to oxygen atoms of bridging COO groups. As a result, all the exchange couplings though carboxylate groups (see Figure 7) should be consistent, a priori, to be operative. In fact, under the influence of zero-field splitting, the d_{z^2} orbital is stabilized with respect to the $d_{x^2-y^2}$ one (the fit indicates a splitting of 15 K) so that, at low temperature, the relevant exchange pathways are along Cu(1′)–Cu(3) and Cu(3)–Cu(2) (B–C′ and A–B pathways, respectively). The significant difference among the respective J values is likely to be related to the role played by the exchange-propagating orbitals of the bridging COO groups.

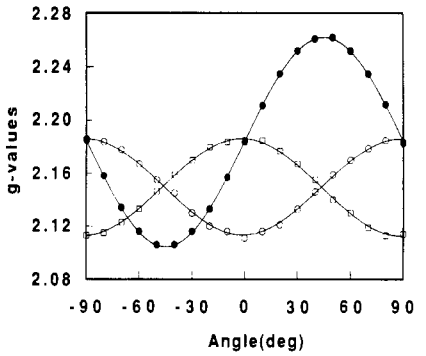

Figure 8. Angular dependences of the g-values of a single crystal of the $[Cu_3,Cu_2]$ compound: (●) *cac*; (○) *aba*; (□) *bcb*.

Electron Paramagnetic Resonance. The polycrystalline powder EPR spectra of $[Cu_3,Cu_2]$ samples show a relatively broad axial-type signal ($\Delta H_{pp} = 90$ G) nearly independent of the temperature, yielding $g_\parallel = 2.25$ and $g_\perp = 2.10$. The corresponding G parameter, defined as $(g_\parallel - 2)/(g_\perp - 2)$ is 2.5, much lower than 4, this suggesting that the experimental g-values do not correspond to molecular ones. This is fully confirmed by single-crystal experiments carried out on a prismatic crystal having the (±1,0,0), (0,±1,0), and (0,0,±1) faces well developed. Since the monoclinic β angle is 90.99°, we can consider (within the experimental error) that the crystal was rotated around three orthogonal axes parallel to the crystallographic ones. There are three magnetically nonequivalent Cu(II) chromophores in the unit cell. Thus, three signals should be expected in every plane. However, only one signal is observed, indicating exchange interactions between the Cu(II) polyhedra. The experimental results (Figure 8) afford g-values of $g_\parallel = 2.26$ and $g_\perp = 2.10$, in excellent agreement with the polycrystalline powder spectra.

The angular dependence of the signals indicates that $g_\parallel$ and one component of $g_\perp$ are located in the *ac* plane, making angles of 45° with the *a* and *c* axes. The remaining $g_\perp$ component is parallel to the *b* axis. On the other hand, the angular variation of the line width is not significant (60 ± 15 G), which makes difficult any new consideration about the magnetic dimensionality of the system.

EPR results on nickel-containing samples are poorer. Room-temperature spectra present only one weak and broad ($\Delta H_{pp} =$ 2000 G) signal centered at $g = 2.30$, which is not resolved at lower temperatures, this precluding any reliable analysis.

Concluding Remarks

The isostructural compounds $Cu_3[M(cdta)]_2(NO_3)_2 \cdot 15H_2O$ (M = Cu, Ni) described here are actually the limits of a solid solution of composition $Cu_3[Cu_{1-x}Ni_x(cdta)]_2(NO_3)_2 \cdot 15H_2O$ ($0 \le x \le 1$). In this series, the copper compound $[Cu_3,Cu_2]$ constitutes a nice example illustrating Hathaway's plasticity concept.[22] In fact, the coordination environments of the three crystallographically independent copper atoms are all different.

From the magnetochemical point of view, the newness of the resulting one-dimensional lattice must be stressed. This one is built up of three magnetic sublattices connected through three different interactions. In this context, the $[Cu_3,Cu_2]$ compound

(21) Hendrickson, D. N. In *Magneto-structural Correlations in Exchange Coupled Systems*; NATO ASI Series; Reidel: Dordrecht, Holland, 1985; p 253.

(22) Hathaway, B. J. *Struct. Bonding* **1984**, *57*, 55.

can be considered as the first edta-like metalate where the proper topology of the lattice should result in one-dimensional ferrimagnetism. Nevertheless, the weakness of the Cu–Cu interactions renders difficult the experimental observation of the predicted behavior and new experiments at very low temperatures are needed in order to confirm this hypothesis.

Once more time, the results described in this work evidence the usefulness of edta-like ligands to get ideal model systems to explore low-dimensional ferrimagnetic behavior. Although the above mentioned difficulties have partly limited our success in this case, the features of this series, by widening even more the structural richness of this kind of metalate, open new perspectives to stabilizing 1-D ferrimagnets.

Supplementary Material Available: Tables S1–S8, listing physical properties and main data relating to structure determination, atomic coordinates, thermal parameters, hydrogen positions, and bond distances and angles for compounds **1** and **2**, Tables S9–S11, listing twisting angles and asymmetry parameters for carboxylates and least-squares planes for compounds **1** and **2**, and Table S12, listing the expressions for the transfer matrix elements (19 pages). Ordering information is given on any current masthead page.